Nonlinear control of coherent absorption and its optical signal processing applications Ⓕ

Angelos Xomalis ⓘD, Yongmin Jung, Iosif Demirtzioglou ⓘD, Cosimo Lacava ⓘD, Eric Plum ⓘD, David J. Richardson ⓘD, Periklis Petropoulos ⓘD, and Nikolay I. Zheludev ⓘD

COLLECTIONS

Ⓕ   This paper was selected as Featured

View Online   Export Citation   CrossMark

ARTICLES YOU MAY BE INTERESTED IN

Improved control of nonlinear absorption advances all-optical signal processing
Scilight **2019**, 431105 (2019); https://doi.org/10.1063/10.0000194

Cryptography in coherent optical information networks using dissipative metamaterial gates
APL Photonics **4**, 046102 (2019); https://doi.org/10.1063/1.5092216
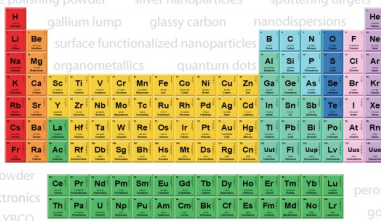
Attosecond pulse metrology
APL Photonics **4**, 080901 (2019); https://doi.org/10.1063/1.5086773

Nonlinear control of coherent absorption and its optical signal processing applications

View Online   Export Citation   CrossMark

Angelos Xomalis,[1,2,a),b)] Yongmin Jung,[1] Iosif Demirtzioglou,[1] Cosimo Lacava,[1] Eric Plum,[1,2,a)]
David J. Richardson,[1] Periklis Petropoulos,[1] and Nikolay I. Zheludev[1,2,3,a)]

AFFILIATIONS

[1] Optoelectronics Research Centre, University of Southampton, Highfield, Southampton SO17 1BJ, United Kingdom
[2] Centre for Photonic Metamaterials, University of Southampton, Highfield, Southampton SO17 1BJ, United Kingdom
[3] Centre for Disruptive Photonic Technologies, SPMS, TPI, Nanyang Technological University, Singapore 637371, Singapore

[a)] Authors to whom correspondence should be addressed: ax210@cam.ac.uk; erp@orc.soton.ac.uk; and niz@orc.soton.ac.uk
[b)] Present address: NanoPhotonics Centre, Cavendish Laboratory, University of Cambridge, Cambridge CB3 0HE, United Kingdom.

ABSTRACT

All-optical data processing continues to attract significant interest as a way to overcome the electronic signal processing bottleneck of fiber telecommunication networks. Nonlinear optical devices such as limiters and saturable absorbers rely on intensity-dependent attenuation of light. However, making such devices using intensity-dependent multiphoton dissipation processes is an issue as these make complete absorption and transmission impossible. Here, we show that nonlinear phase retardation in an optical fiber can control the dissipation of coherent light waves interacting on a thin plasmonic absorber from total absorption to perfect transmission. The fiber's instantaneous Kerr nonlinearity and the femtosecond coherent absorption time scale make this approach ultrafast. We report proof-of-principle demonstrations of all-optical intensity discrimination, power limiting, pulse restoration, pulse splitting, and signal transfer between carrier wavelengths within a fiber circuit. Our results indicate that nonlinear control of coherent absorption can imitate and outperform saturable and multiphoton absorption in terms of bandwidth and contrast.

I. INTRODUCTION

Since 1926, when nonlinear optics began to develop with the observation of nonlinear absorption in uranium-doped glass,[1] saturable absorption and multiphoton absorption have become the basis of applications from laser physics to signal processing, microfabrication, and imaging. Semiconductors,[2] quantum dots,[3] carbon nanotubes,[4,5] and doped fibers[6] have been used as saturable absorbers for mode-locking and Q-switching of lasers. Multiphoton absorption in photoresists, dyes, and metamaterials is the basis of direct laser writing,[7,8] imaging through biological tissue,[9] optical limiting, and all-optical signal processing.[10,11] However, conventional saturable and multiphoton absorption suffer from some fundamental limitations. Saturable absorption cannot eliminate absorption completely as it is a consequence of absorption-induced depletion of a material's ground state. Similarly, multiphoton absorption causes a gradual intensity reduction that reduces its own efficiency, making the effect self-limiting and preventing complete absorption.

Here, we introduce nonlinear coherent perfect absorption, which exploits an intensity-dependent optical phase shift to control the absorption of light waves with strong phase correlation interacting with a thin absorber. This, in principle, allows nonlinear control of dissipation within an ideal absorber from perfect transmission to perfect absorption. After introducing this nonlinear absorption mechanism for continuous wave (CW) light under ideal conditions (Fig. 1), we demonstrate it in a fiber-based Sagnaclike interferometer, where self-phase modulation (SPM) and cross-phase modulation (XPM) in a nonlinear optical fiber yield intensity-dependent phase shifts and a 70-nm-thick plasmonic metamaterial fabricated on the core of a cleaved optical fiber acts as the absorber. First, we study the intensity-dependence of nonlinear coherent absorption
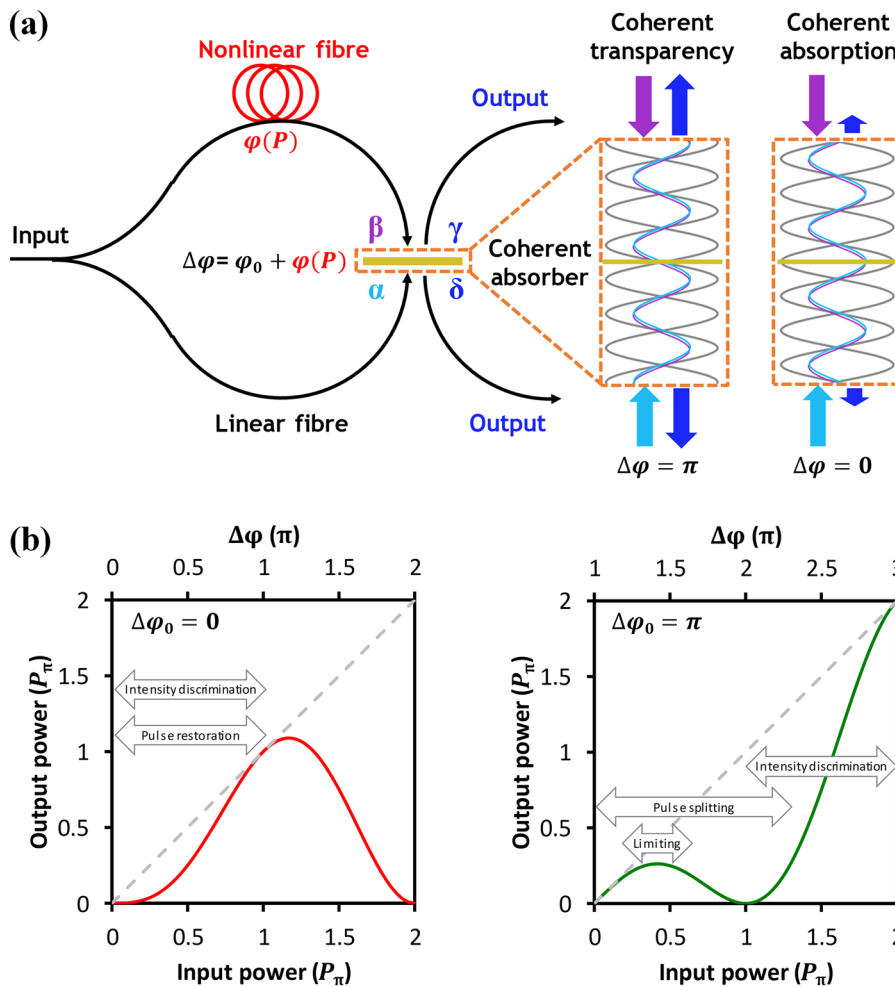
FIG. 1. Control of coherent absorption with nonlinearity. (a) Counterpropagating and co-polarized light waves with strong phase correlation, α and β, form a standing wave of electric energy density. At high optical power P, propagation of the light wave β through a Kerr medium (nonlinear fiber) yields a nonlinear phase shift $\varphi(P)$ that displaces the standing wave's nodes and antinodes. A thin absorber located at a standing wave node (antinode) causes weak (strong) light absorption known as coherent transparency (coherent absorption). Therefore, absorption is controlled by the phase difference $\Delta\varphi$ of α and β on the absorber, which is the sum of the phase φ_0 associated with the length difference of the interferometer arms and the nonlinear phase $\varphi(P)$. (b) Dependence of the total output power of waves γ and δ on the total input power of waves α and β for an ideal absorber. Characteristic cases of $\varphi_0 = 0$ and $\varphi_0 = \pi$ are shown, where P_π is the total input power that introduces a nonlinear phase shift of π between α and β. Dashed lines indicate 100% transmission for comparison.

with optical pulse trains, and then, we measure its effect on individual pulses. We observe intensity discrimination and optical limiting (Fig. 2), narrowing and splitting of few-picosecond optical pulses (Fig. 3), and signal transfer between different carrier wavelengths (Fig. 4).

II. COHERENT ABSORPTION

The light-matter interaction of a material of substantially subwavelength thickness can be controlled by counterpropagating coherent light waves (α and β). This allows the manifestation of the thin film's linear[12] and nonlinear[13] optical properties to be controlled. Here, we consider linear absorption of such a lossy thin film, which can be controlled, in principle, from 0% to 100% [Fig. 1(a)].[12] Ideal performance can be achieved with a "coherent perfect absorber," which exhibits both 25% transmission and reflection and 50% absorption for illumination from one side only. Almost ideal coherent absorbers consisting of metamaterials,[12] multilayer graphene,[14] heavily doped silicon films,[15] and other materials have been reported. The limiting cases of low and high absorption

are known as coherent transparency (CT) and coherent absorption (CA). Destructive interference of both waves, α and β, on an absorber of negligible thickness results in perfect transparency since light-matter interaction is prevented by electric field cancellation. Constructive interference of both incident waves causes enhanced absorption due to the interaction of the absorber with an enhanced electric field.

We note that this phenomenon can also be understood in terms of output waves (γ and δ) formed by the interference of the transmission of one incident wave with the reflection of the other, i.e., $E_\gamma = tE_\alpha + rE_\beta$ and $E_\delta = tE_\beta + rE_\alpha$, where E is the electric field, and a coherent perfect absorber is described by a transmission coefficient $t = 0.5$ and a reflection coefficient $r = -0.5$. This simplifies to $E_\gamma = -E_\delta$, indicating that the resulting output waves always have equal amplitudes. In particular, equal input fields yield zero output fields (coherent absorption), while copolarized input fields of equal magnitude and opposite phase yield output fields that are identical to the input fields (coherent transparency).

For illumination of an ideal coherent absorber with copolarized mutually coherent input signals of the same intensity, the total

output power P_{out} is given by the total input power P_{in} and the phase difference $\Delta\varphi$ between the input signals,

$$P_{out} = P_{in} \sin^2\left(\frac{\Delta\varphi}{2}\right). \tag{1}$$

Such optical devices with two inputs (α and β) and two outputs (γ and δ) can perform all-optical signal processing functions.[16] As coherent control of absorption of light with light is compatible with single photons[14] and offers THz bandwidth in fiber-optic configurations,[17] it has the potential to underpin quantum and energy-efficient, high-bandwidth all-optical signal processing applications.

III. NONLINEAR CONTROL OF COHERENT ABSORPTION

We show how coherent transparency and coherent absorption of a thin linear absorber can be exploited to achieve nonlinear coherent absorption. Nonlinear absorption will occur if the optical power P controls the interference of the input signals on the thin absorber. This will be the case if one of the input signals, e.g., β, experiences a nonlinear phase shift $\varphi(P)$ due to propagation through a medium with a non-linear refractive index, i.e., a Kerr-medium, see Fig. 1(a). The resulting power-dependent phase difference between α and β on the thin absorber will be

$$\Delta\varphi = \Delta\varphi_0 + \varphi(P), \tag{2}$$

where $\Delta\varphi_0$ is the phase difference at low power and is determined by the optical length difference of the interferometer arms. Following from Eq. (1), with increasing power, the nonlinear phase shift will give rise to a variation between coherent transparency (at $\Delta\varphi = \pm\pi, \pm3\pi, \ldots$) and coherent absorption (at $\Delta\varphi = 0, \pm2\pi, \ldots$), respectively, corresponding to 0% and 100% absorption within an ideal thin absorber. For a given intensity range, the effect may thus be exploited for preferential absorption of either low intensities (intensity discrimination) or high intensities (optical limiting) by choosing $\Delta\varphi_0$ and the nonlinearity of the Kerr-medium accordingly [Fig. 1(b)].

Here, we use a highly nonlinear optical fiber (HNLF) as the Kerr-medium and a nanostructured plasmonic metamaterial as the thin absorber. Using self-phase modulation in the nonlinear fiber to control absorption in the metamaterial, we demonstrate optical limiting and intensity discrimination as well as picosecond (ps) pulse restoration and shaping. Exploiting cross-phase modulation, we demonstrate all-optical transfer of pulses of a few picosecond duration from one carrier wavelength to another. All of our experiments were conducted in a polarization-maintaining optical fiber network containing a fully fiberized coherent absorber and a nonlinear optical fiber.

The absorber is a plasmonic metasurface on the core of an optical fiber. It was fabricated on the cleaved end of a single-mode polarization-maintaining optical fiber with about 10 μm mode diameter, coupled to a second cleaved polarization-maintaining optical fiber using two microcollimator lenses and packaged with fiber micro ferrules in an aluminum enclosure to create an in-line fiber metadevice with standard pigtail connectors as described in Ref. 16. The fiber metamaterial is an array of asymmetric split ring apertures with unit cell dimensions of 700 × 700 μm² that was milled

into a 70-nm-thick gold film by focused ion beam milling, where the unit cell's symmetry axis is aligned with the slow axis of the fiber. At the operation wavelength of 1550 nm, for input signals α(β), the metadevice has 24% (24%) transmission, 18% (8%) reflection, and 58% (68%) absorption including coupling losses. We estimate the damage threshold of the metamaterial absorber to be a few milliwatts average power and note that this could be increased by fabricating the absorber on a larger mode-area fiber.

The polarization-maintaining highly nonlinear fiber (HNLF from OFS Fitel LLC) has a length of 493 m, an effective nonlinear coefficient of $\gamma_{NL} = 10.7$ (W km)$^{-1}$, a zero dispersion wavelength of 1544 nm, and a dispersion slope of 0.029 ps/(nm² km). We exploit the nonlinear phase shift induced on and by laser pulses propagating through the nonlinear optical fiber to control absorption in the plasmonic metamaterial absorber. Neglecting the effects of chromatic dispersion in the fiber, the nonlinear phase shift φ_{SPM} experienced by a laser signal of power P due to self-phase modulation (SPM)[18] is

$$\varphi_{SPM}(P) = \gamma_{NL}L_{eff}P, \tag{3}$$

where the fiber's nonlinear coefficient $\gamma_{NL} = \frac{2\pi n_2}{\lambda_0 A_{eff}}$, which describes the nonlinear phase shift per unit length and power, is derived from the intensity-dependent refractive index $n = n_0 + n_2 I$ of the Kerr medium. These expressions depend on the linear refractive index n_0, nonlinear refractive index n_2, intensity $I = P/A_{eff}$, effective mode area $A_{eff} = 12.5$ μm², free-space wavelength λ_0, nonlinear effective length $L_{eff} = (1 - e^{-\alpha L})/a$, and propagation loss of the nonlinear fiber $a = 0.79$ dB/km. Cross-phase modulation (XPM)[18] will introduce a phase shift φ_{XPM} on a co-propagating signal of the same polarization at a different wavelength of

$$\varphi_{XPM}(P) = 2\varphi_{SPM}(P). \tag{4}$$

As the Kerr nonlinearity is instantaneous and coherent absorption occurs on a time scale of 10 fs,[19] nonlinear control of coherent absorption can, in principle, offer 100 THz bandwidth in low-dispersion environments. It is characterized by the power it takes to introduce a phase shift of π in the Kerr nonlinear element to go from coherent absorption to coherent transmission. Self-phase modulation of π requires a power of 620 mW entering our nonlinear fiber. This corresponds to a saturation intensity of 5 MW/cm² in the nonlinear fiber core. Thus, a 1 ps pulse with 5 μJ/cm² fluence will saturate absorption in our device. For comparison, commercial saturable absorbers (BATOP GmbH),[20] are characterized by larger saturation fluences of about 200 μJ/cm² and take a longer relaxation time ranging from 0.5 to 30 ps to recover.

All experiments were performed in a polarization-maintaining fiber-loop interferometer using linearly polarized laser light with the electric field oriented parallel to the symmetry axis of the metamaterial unit cell. Our implementations are similar to a nonlinear optical loop mirror (NOLM)[21] and other related devices such as a Nonlinear Amplifying Loop Mirror (NALM)[22] and a Terahertz Optical Asymmetric Demultiplexer (TOAD).[23] However, in contrast to a typical NOLM and its variants, we combine the signals α and β on a thin absorber (rather than a lossless coupler). Our use of a thin absorber rather than a lossless coupler makes both the physical mechanism of light modulation and the resulting relationship between the interferometer output signals different from a NOLM and related devices.

A NOLM and its variants act as a nonlinear beam splitter, where interference controls how energy is distributed between the outputs of a coupler, resulting in complementary interferometer output signals (e.g., one at maximum, while the other is at minimum). In contrast, our implementation acts as a nonlinear absorber, where interference controls how much energy is dissipated in a thin absorber, resulting in identical output signals (e.g., both at maximum or both at minimum), when perfectly realized.

The absorber is placed outside the loop, allowing interferometer arms of different length and thus control over $\Delta\varphi_0$. The interferometer is stable on subsecond time scales, which is sufficient for proof-of-principle demonstrations. A gradual phase drift at longer time scales was exploited for switching between different characteristic cases of nonlinear coherent absorption. The laser sources in all experiments are fiber-coupled tunable CW lasers (ID Photonics CoBrite-DX4) operating at wavelengths of either 1550 nm or 1531 nm as specified below. Laser pulses were generated by launching one of these sources into a frequency comb generator (OptoComb LP-5011) that generates picosecond pulses at a repetition rate of 10 GHz, which were filtered to adjust the pulse shape and duration. In order to achieve sufficient power levels, we used

erbium-doped fiber amplifiers (KEOPSYS) that were protected from back-reflections using optical isolators.

IV. INTENSITY DISCRIMINATION AND OPTICAL LIMITING

In order to demonstrate preferential absorption of either high or low intensity light, we exploited self-phase modulation in the fiber-optic network shown in Fig. 2(a). Rather than using CW laser light (as in Fig. 1), we conducted our experiments with laser pulses to achieve substantial nonlinear phase shifts at low average power. We generated 1.9 ps pulses with 10 GHz repetition rate at the 1550 nm telecom wavelength. The pulse train envelope was shaped into a sawtooth waveform with 1 MHz repetition rate using an intensity electro-optic modulator (EOM) (EOSPACE AX-0K5-10-PFA-PFA-UL) controlled by an arbitrary waveform generator (Tektronix AWG7122C) to conveniently measure the nonlinear absorption as a function of input pulse peak power. Then, the signal was split between the counterpropagating arms of a Sagnaclike interferometer. The same nonlinear fiber was part of both interferometer arms, where different nonlinear phase shifts resulted from an attenuator (power attenuation to ~3.5%) imposing different peak powers of the
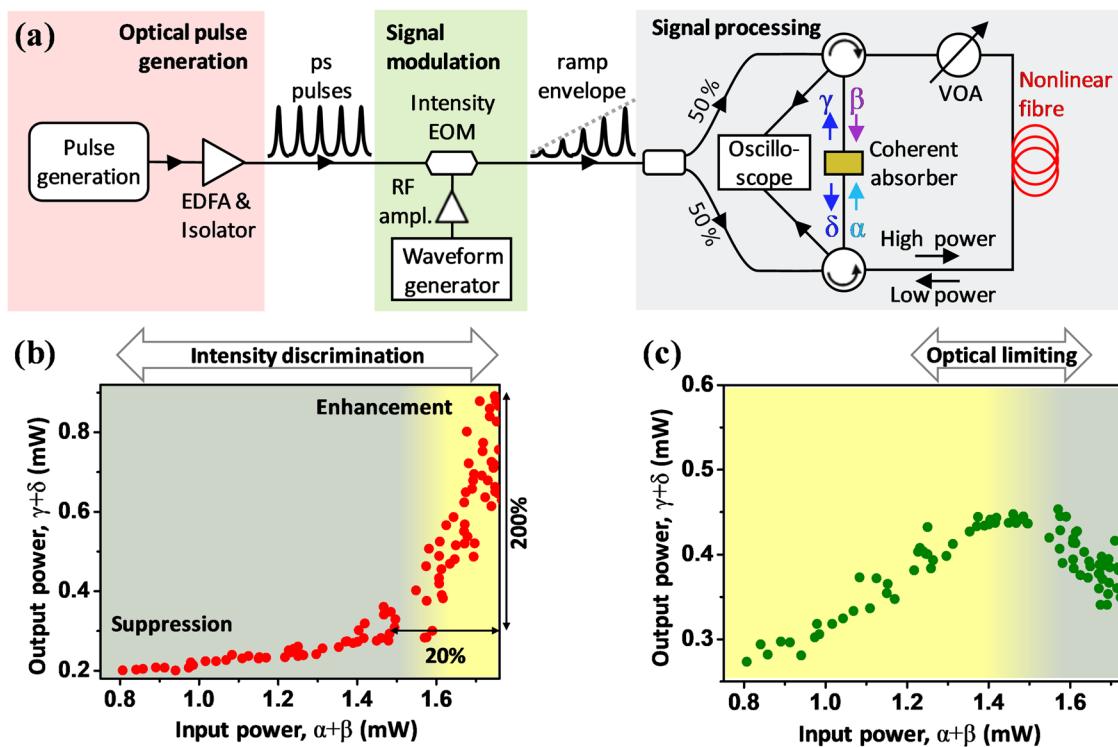
FIG. 2. Intensity discrimination and optical limiting. (a) Experimental setup where nonlinear coherent absorption arises from self-phase modulation of optical pulses interacting on a plasmonic metamaterial coherent absorber. The pulses have 1.9 ps duration and 1550 nm wavelength. EDFA—Erbium Doped Fiber Amplifier, EOM—Electro-Optic Modulator, and VOA—Variable Optical Attenuator. [(b) and (c)] Measurements of coherent absorber pulse-average output power (summed power of γ and δ) as a function of its pulse-average input power (α and β). (b) Suppression of low-power input signals by coherent absorption ($\Delta\varphi \approx 0$, gray) transitions towards relative enhancement of high-power input signals by coherent transmission (yellow) as $\Delta\varphi$ approaches π. (c) Coherent transmission ($\Delta\varphi \approx \pi$) of low power input signals transitions towards coherent absorption of high-power input signals as $\Delta\varphi$ approaches 0 resulting in optical limiting.

counterpropagating signals α and β within the nonlinear fiber. The resulting beams were then recombined on the coherent absorber with an intensity-dependent phase difference due to self-phase modulation. An optical delay line in one interferometer arm (not shown in the figure) was used to ensure that the pulses arrive simultaneously on the metamaterial absorber. Attenuation of the absorber input signals to submilliwatt average power protected the metamaterial from optical damage, where input signals with equal power, α = β, were used to maximize the efficiency of coherent absorption. The pulse train envelopes of the outputs γ and δ were detected simultaneously via circulators using an oscilloscope with built-in photodetectors (Agilent Infiniium DCA-J 86100C) and the inputs α and β were characterized in the same way. Note that the detection system used in these experiments was chosen to reliably measure the output pulse train envelope to determine the overall nonlinear response of the device to the sawtooth modulated input. Consequently, pulse shaping at the individual picosecond pulse level is not resolved in this experiment (but is studied later). We therefore refer to powers in these measurements, which resolve pulse train envelopes but average over individual picosecond pulses, as "pulse-average powers."

There are two limiting cases of nonlinear coherent absorption that are illustrated in Figs. 2(b) and 2(c) in terms of pulse-average output power as a function of pulse-average input power of the coherent absorber metadevice. A 620 mW change of the differential peak power of pulses propagating along the nonlinear fiber, causing a nonlinear phase change of π at the pulse peak, corresponds to a change in pulse-average power of about 0.7 mW (α + β) entering the metadevice in Fig. 2. If the input optical signals α and β constructively interfere on the thin absorber at low intensities, resulting in high absorption, the nonlinear phase shift with increasing intensity will reduce absorption, mimicking saturable absorption, Fig. 2(b). Large absorption of low-power input and weak absorption of high-power input provides intensity discrimination (contrast enhancement). We observe that a 20% change in input pulse-average power (between 1.5 and 1.8 mW) yields a 200% change in output pulse-average power (between 0.3 and 0.9 mW). On the other hand, if the optical signals destructively interfere at low intensities resulting in low absorption, then the nonlinear phase shift resulting from increased intensity will increase absorption, mimicking multiphoton absorption and providing an optical limiting functionality, Fig. 2(c). In this case, we observe that the output pulse-average power peaks for a 1.45-mW input pulse-average power and then decreases for a further increase in input power. We note that optical pulses (other than ideal rectangular pulses) have an intensity that varies across the pulse shape, which leads to a nonlinear phase shift that varies across the pulse and that will lead to a variation of the coherent absorption of the low-intensity and high-intensity features across the pulse which will be explored in more detail below. Therefore, optical limiting results in partial absorption of Gaussian pulses, explaining why the detected pulse-average power does not (and should not) go to zero in our experiments. In addition, an ideal coherent absorber would be required for complete absorption, e.g., for complete suppression of coherent low-power input light [Fig. 1(b)]. A small background in our measurements [Figs. 2(b) and 2(c)] is caused by the presence of amplifiers in our setup. Nevertheless, the observed relationships of output on input pulse-average power closely resemble those expected for true CW signals

interacting on an ideal coherent absorber in a nonlinear interferometer [Fig. 1(b)]. The theoretical graphs [Fig. 1(b)] show how, depending on the initial phase shift φ_0, an additional nonlinear phase shift due to increasing input power yields either a reduction or an increase in overall absorption, and this is what is observed experimentally [Figs. 2(b) and 2(c)].
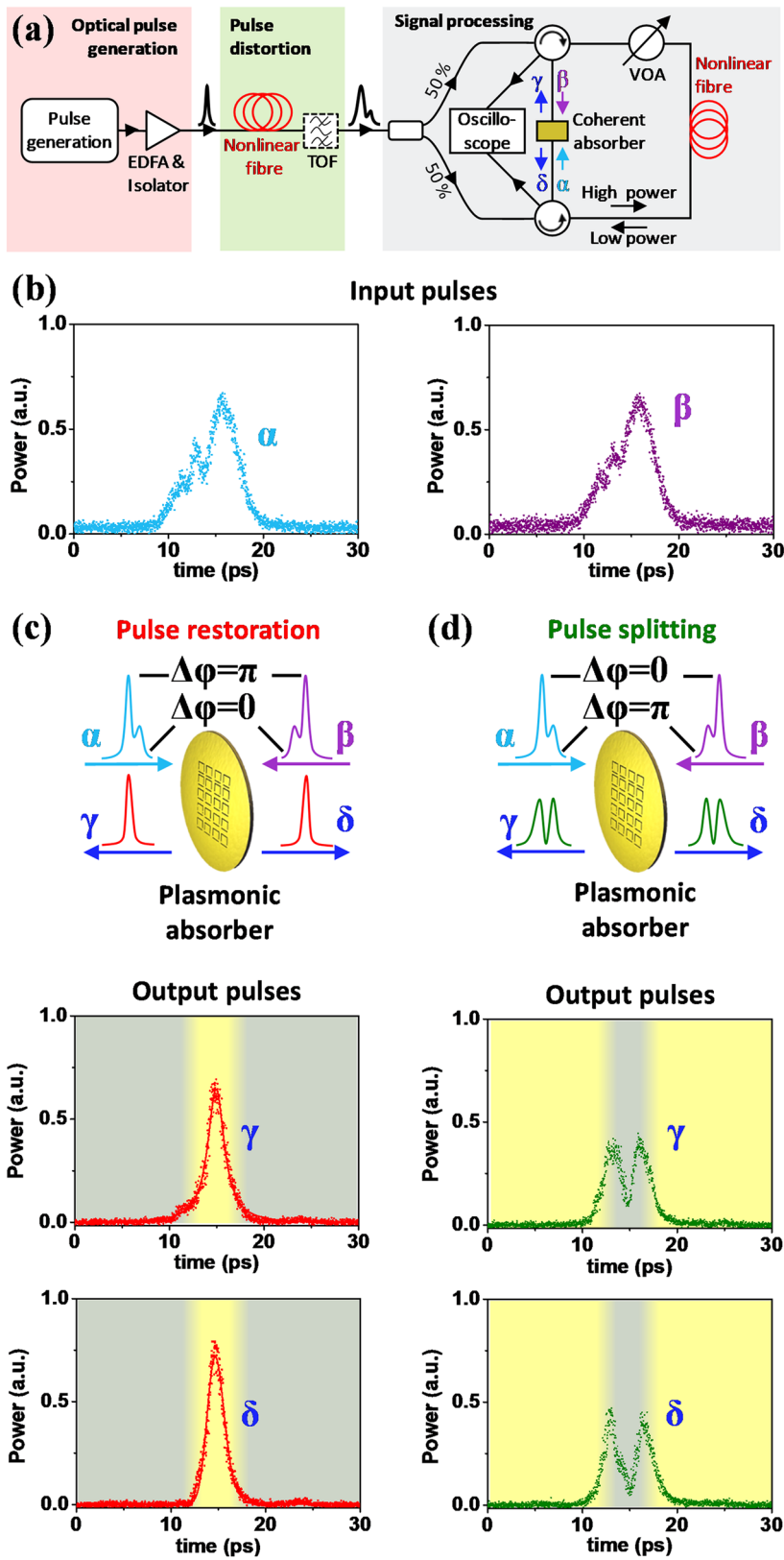
V. PULSE RESTORATION AND PULSE SPLITTING

Preferential absorption of either low or high power may be exploited for optical pulse shaping, such as restoration/narrowing or splitting of pulses. In order to demonstrate this, we replaced the electro-optic modulator in Fig. 2(a) with an additional polarization-maintaining nonlinear fiber (HNLF from OFS Fitel LLC) of 299 m length with an effective nonlinear coefficient γ_{NL} = 10.4 (W km)$^{-1}$ and dispersion of −0.4 ps/(nm km) at 1550 nm wavelength with a slope of 0.026 ps/(nm^2 km). The amplified laser pulses were spectrally broadened through self-phase modulation in the normally dispersive highly nonlinear fiber, and subsequently filtered in a tunable passband filter set to about 3 nm bandwidth, see Fig. 3(a). The combination of self-phase modulation, dispersion, and filtering distorted the pulses in the time domain, broadening their duration and generating the features shown in Fig. 3(b). The metadevice input and output pulses were amplified (KEOPSYS Erbium-doped fiber amplifiers) for detection just prior to being recorded with a fast optical sampling oscilloscope (EXFO PSO-102). Here, the average power in each metadevice input channel, α and β, was ~0.4 mW.

The distorted input pulses had a full width at half maximum of 5.8 ps [Fig. 3(b)]. As the low and high power components of these pulses accumulate different nonlinear phase shifts in the nonlinear fiber, they may be selectively transmitted or absorbed by the coherent absorber. Suppression of low power by coherent absorption results in pulse narrowing and removal of low-power pulse distortions, while the higher power component of the pulse is transmitted [Fig. 3(c)]. We observed an almost 3-fold pulse width reduction from 5.8 ps to 2.1 ps. In contrast, complete suppression of high power by coherent absorption, while lower power is (partially) transmitted, splits a single input pulse into a pair of consecutive bright output pulses by creating a dark pulse in between [Fig. 3(d)]. In each case, we observed almost identical output signals, γ and δ.

VI. SIGNAL TRANSFER BETWEEN CARRIER WAVELENGTHS

Nonlinear coherent absorption can also be used to transfer intensity modulation from one optical wavelength to another as different optical signals co-propagating along the same nonlinear fiber modulate each other's phase by cross-phase modulation, which then controls their absorption within the coherent absorber. In order to demonstrate this, we combined ~10 ps pump laser pulses at 1531 nm wavelength propagating along one interferometer arm with 1550 nm continuous wave (CW) probe laser light propagating along both interferometer arms,[24] as illustrated by Fig. 4(a). The pump pulses are injected before the nonlinear fiber and filtered out thereafter. A polarization controller and polarization beam splitter were used to ensure that the pump pulses entering the interferometer had the same polarization as the probe light (with the electric field parallel

FIG. 3. Pulse restoration and pulse splitting. (a) Experimental setup where nonlinear coherent absorption arises from self-phase modulation of distorted optical pulses of 1550 nm wavelength interacting on a plasmonic metamaterial coherent absorber. EDFA— Erbium Doped Fiber Amplifier, TOF—Tuneable Optical Filter, and VOA—Variable Optical Attenuator. [(b)–(d)] Amplitude profiles of (b) input pulses α (left) and β (right) entering the coherent absorber device and [(c) and (d)] output pulses γ (top) and δ (bottom) leaving the device. In channel β, the low and high power pulse components accumulate different nonlinear phase shifts through interaction with the nonlinear fiber. When a pulse in channel β interacts on the coherent absorber with a pulse in channel α (that does not undergo nonlinear transformation), the high and low intensity components of the pulses experience different levels of absorption. Tuning the initial phase shift between the channels and the amount of intensity-dependent phase shift in the fiber, one can realize two limiting cases: (c) preferential absorption of low-power pulse components resulting in pulse narrowing/restoration and (d) preferential absorption of high-power pulse components resulting in pulse splitting. Coherent absorption (gray) occurs for pulse components interacting on the coherent absorber with a phase difference of $\Delta\varphi \approx 0$, while coherent transmission (yellow) occurs for $\Delta\varphi \approx \pi$.
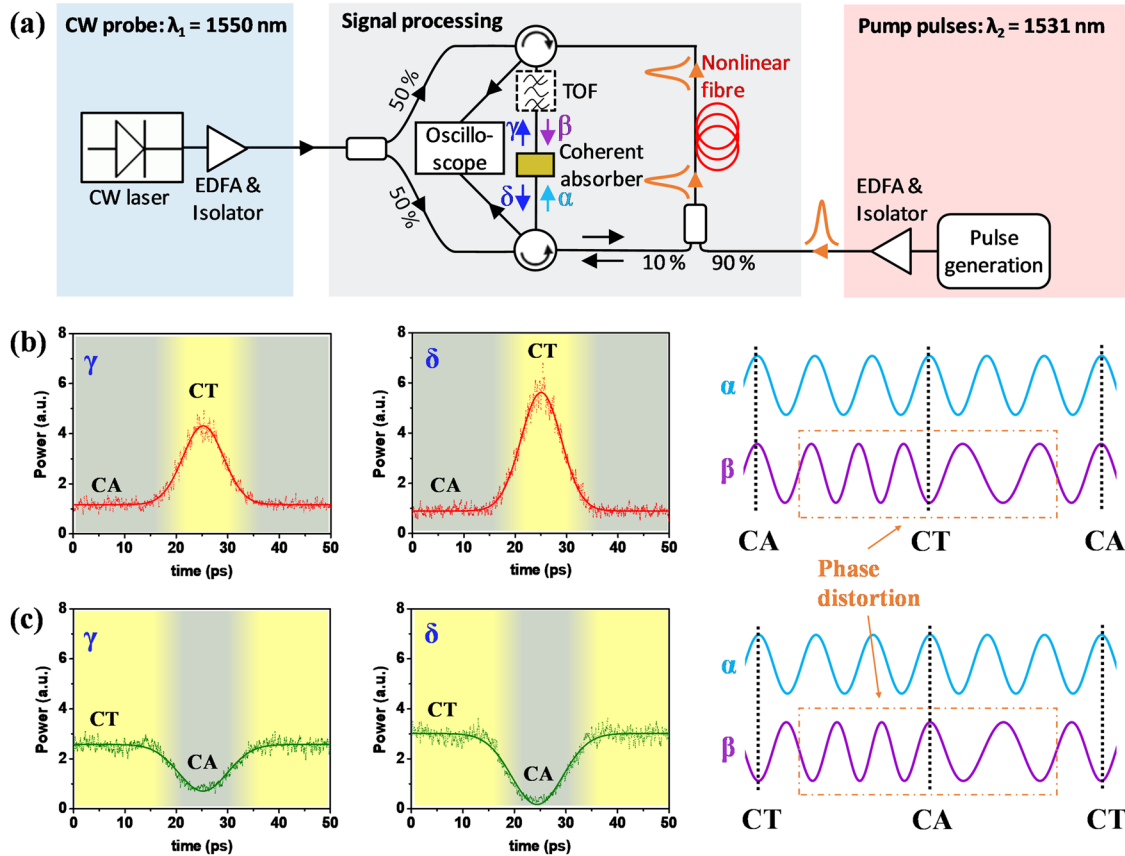
FIG. 4. Signal transfer between wavelengths. (a) Experimental setup where nonlinear coherent absorption of 1550 nm CW probe light on a plasmonic metamaterial absorber is controlled by cross-phase modulation in a nonlinear fiber caused by 1531 nm wavelength laser pulses. EDFA—Erbium Doped Fiber Amplifier, TOF—Tuneable Optical Filter. [(b) and (c)] Time traces of the probe output channels (γ and δ) where a pump-induced nonlinear phase distortion of probe input wave β leads to (b) increased transmission (yellow) and (c) increased absorption (gray) on the metamaterial absorber. The schematics illustrate how the nonlinear phase distortion affects the interference of the probe input waves α and β on the metamaterial absorber. Constructive interference results in coherent absorption (CA), while destructive interference results in coherent transmission (CT).

to the symmetry axis of the metamaterial unit cell). Within the non-linear fiber, the presence of a pump pulse causes an instantaneous refractive index change that is proportional to the instantaneous light intensity (Kerr effect). Therefore, CW light that propagates together with a laser pulse along the nonlinear fiber experiences a phase shift according to Eq. (4). The pump pulse peak power in the nonlinear fiber was 77 mW, implying $\pi/4$ cross-phase modulation. This controls CW light absorption when the interferometer arms, that contain probe light without (α) and with (β) such phase modulation, recombine on the coherent absorber device. The CW probe power entering the nonlinear fiber within the two interferometer arms was much lower, 18.5 mW and 1.4 mW for α and β, respectively, where the difference arises from the 90:10 splitter that injects the pump pulses into the loop. The probe power was attenuated at the metamaterial absorber device inputs to protect the metamaterial from optical damage. Here, the power spectral density of both channels was matched at 1550 nm wavelength, resulting in slightly different average probe powers of 69 μW and

78 μW for α and β, respectively, as phase-modulation of β introduces additional modulation-induced sidebands that are not present in α. The metadevice outputs were amplified (KEOPSYS Erbium-doped fiber amplifiers) and detected with a fast optical sampling oscilloscope (EXFO PSO-102).

Figures 4(b) and 4(c) show the coherent absorber outputs, γ and δ, for the characteristic cases, where a nonlinear phase shift of about $\pi/4$ caused by a pump pulse with about 77 mW peak power decreases [panel (b)] or increases [panel (c)] coherent absorption of probe light. In the case of Fig. 4(b), probe light is coherently absorbed, except when a pump-pulse-induced phase modulation makes the coherent absorber (partially) transparent, resulting in bright output pulses, γ and δ, at the probe wavelength. In the case of Fig. 4(c), probe light is (partially) transmitted, except when a pump-pulse-induced phase modulation triggers coherent absorption, resulting in dark output pulses within the CW background at the probe wavelength. These observations demonstrate the transfer of 10 ps pulses into bright or dark pulses between telecommunications

wavelengths with a spectral separation of 19 nm and at least 100 GHz bandwidth.

VII. CONCLUSIONS

To conclude, we have demonstrated a new all-optical mechanism for controlling absorption of coherent light and its use for signal processing. The nonlinear effect results from interaction of counterpropagating mutually coherent light waves on a thin absorber with an intensity-dependent phase difference. We have demonstrated nonlinear coherent absorption in a fiber-based interferometer, where intensity-dependent phase shifts occur in an optical fiber with Kerr nonlinearity and absorption occurs in a fiberized plasmonic metamaterial absorber. We exploit the nonlinearity to perform nonlinear all-optical signal processing functions, including all-optical limiting, 10-fold contrast enhancement between different power levels, as well as restoration, narrowing, and splitting of 5.8 ps pulses and transfer of optical signals between different telecommunications wavelengths with at least 100 GHz bandwidth. We argue that nonlinear control of coherent absorption can potentially provide all-optical solutions for optical telecommunications and data processing, where limiting prevents optical damage, better optical contrast increases data capacity in classical[25] and quantum[26] channels, signal regeneration enables long transmission lines, and signal transfer between different wavelength division multiplexing (WDM) channels is essential. As the Kerr effect is instantaneous and coherent absorption occurs on a time scale of 10 fs,[19] up to 100 THz bandwidth may be achievable in low-dispersion environments. Beyond absorption, thin films and structured interfaces can perform other optical functions from diffraction, focusing, and holography to polarization control and filtering, which can be controlled by interaction with counterpropagating mutually coherent light waves,[12] implying that any such function would become nonlinear in an interferometer with Kerr nonlinearity as reported here.

ACKNOWLEDGMENTS

REFERENCES

[1] S. J. Wawilow and W. L. Lewschin, Z. Phys. **35**, 920–936 (1926).

[2] U. Keller, K. J. Weingarten, F. X. Kartner, D. Kopf, B. Braun, I. D. Jung, R. Fluck, C. Honninger, N. Matuschek, and J. Aus der Au, IEEE J. Sel. Top. Quantum Electron. **2**, 435–453 (1996).

[3] P. Guerreiro and S. Ten, Appl. Phys. Lett. **71**, 1595–1597 (1997).

[4] S. Y. Set, H. Yaguchi, Y. Tanaka, and M. Jablonski, J. Lightwave Technol. **22**, 51 (2004).

[5] A. Martinez and S. Yamashita, Opt. Express **19**, 6155–6163 (2011).

[6] V. V. Dvoyrin, V. Mashinsky, and E. Dianov, Opt. Lett. **32**, 451–453 (2007).

[7] S. Kawata, H.-B. Sun, T. Tanaka, and K. Takada, Nature **412**, 697 (2001).

[8] G. Kenanakis, A. Xomalis, A. Selimis, M. Vamvakaki, M. Farsari, M. Kafesaki, C. M. Soukoulis, and E. N. Economou, ACS Photonics **2**, 287–294 (2015).

[9] F. Helmchen and W. Denk, Nat. Methods **2**, 932 (2005).

[10] M. Ren, B. Jia, J. Y. Ou, E. Plum, J. Zhang, K. F. MacDonald, A. E. Nikolaenko, J. Xu, M. Gu, and N. I. Zheludev, Adv. Mater. **23**, 5540–5544 (2011).

[11] A. Hayat, A. Nevet, P. Ginzburg, and M. Orenstein, Semicond. Sci. Technol. **26**, 083001 (2011).

[12] E. Plum, K. F. MacDonald, X. Fang, D. Faccio, and N. I. Zheludev, ACS Photonics **4**, 3000–3011 (2017).

[13] S. M. Rao, A. Lyons, T. Roger, M. Clerici, N. I. Zheludev, and D. Faccio, Sci. Rep. **5**, 15399 (2015).

[14] T. Roger, S. Vezzoli, E. Bolduc, J. Valente, J. J. F. Heitz, J. Jeffers, C. Soci, J. Leach, C. Couteau, N. I. Zheludev, and D. Faccio, Nat. Commun. **6**, 7031 (2015).

[15] M. Pu, Q. Feng, M. Wang, C. Hu, C. Huang, X. Ma, Z. Zhao, C. Wang, and X. Luo, Opt. Express **20**, 2246–2254 (2012).

[16] A. Xomalis, I. Demirtzioglou, E. Plum, Y. Jung, V. Nalla, C. Lacava, K. F. MacDonald, P. Petropoulos, D. J. Richardson, and N. I. Zheludev, Nat. Commun. **9**, 182 (2018).

[17] A. Xomalis, I. Demirtzioglou, Y. Jung, E. Plum, C. Lacava, P. Petropoulos, D. J. Richardson, and N. I. Zheludev, Appl. Phys. Lett. **113**, 051103 (2018).

[18] G. Agrawal, *Nonlinear Fiber Optics* (Elsevier Science, 2012).

[19] V. Nalla, J. Valente, H. Sun, and N. I. Zheludev, Opt. Express **25**, 22620–22625 (2017).

[20] See https://www.batop.de/information/SA_infos.html for characteristics of commercially available saturable absorbers.

[21] N. Doran and D. Wood, Opt. Lett. **13**, 56–58 (1988).

[22] M. E. Fermann, F. Haberl, M. Hofer, and H. Hochreiter, Opt. Lett. **15**(13), 752–754 (1990).

[23] J. P. Sokoloff, P. R. Prucnal, I. Glesk, and M. Kane, IEEE Photonics Technol. Lett. **5**(7), 787–790 (1993).

[24] T. Sakamoto, F. Futami, K. Kikuchi, S. Takeda, Y. Sugaya, and S. Watanabe, IEEE Photonics Technol. Lett. **13**, 502–504 (2001).

[25] R.-J. Essiambre, G. J. Foschini, G. Kramer, and P. J. Winzer, Phys. Rev. Lett. **101**, 163901 (2008).

[26] S. Lloyd, Phys. Rev. A **55**, 1613 (1997).